Acta Crystallographica Section B
Structural Science
ISSN 0108-7681

Structure of manganese diacetate tetrahydrate and low-temperature methyl-group dynamics

Béatrice Nicolaï,[a]* Gordon J. Kearley,[b] Alain Cousson,[a] Werner Paulus,[c] François Fillaux,[d] Fabien Gentner,[a] Ludger Schröder[a] and David Watkin[e]

[a]Laboratoire Léon Brillouin (CEA-CNRS), CEA Saclay, 91191 Gif sur Yvette CEDEX, France, [b]Interfacultair Reactor Instituut, UDelft, Mekelweg 15, 2619JB Delft, The Netherlands, [c]Université de Rennes 1, LCSIM/UMR6511, Campus de Bealieu, Avenue du Général Leclerc, 35042 Rennes CEDEX, France, [d]LADIR (CNRS), 2 rue Henry Dunant, 94320 Thiais, France, and [e]Chemical Crystallography Laboratory, 9 Parks Road, Oxford OX1 3PD, England

Correspondence e-mail: nicolai@llb.saclay.cea.fr

Received 13 January 2000
Accepted 19 October 2000

We have determined the crystal structure of manganese(II) diacetate tetrahydrate at 300 and 14 K by single-crystal neutron diffraction. Proton density distributions for each of the three crystallographically distinct methyl groups have been calculated by Fourier difference. At room temperature the observed densities are those of quasi-free rotors. At low temperature rather well localized protons are observed. Inelastic neutron scattering measurements performed with single crystals allow us to assign each of the three tunnelling lines to a particular crystal site. Classical molecular dynamics simulations give density distributions in qualitative agreement with the observations. With quantum mechanics proton distributions can be represented with rotational wavefunctions convoluted with static distributions of librational coordinates. The effective rotational potentials are temperature dependent.

1. Introduction

Light particles experiencing potential functions with topological degeneracy manifest their quantum nature *via* tunnelling. Owing to the spatial extension of the particle wavefunction through the classically forbidden regions, the degenerate ground state in the classical regime splits into sublevels. The magnitude of the tunnel splitting depends on the particle mass and potential shape (distances between identical sites, barrier height *etc.*).

Rotational dynamics of methyl groups give rise to observable tunnelling transitions in many molecular crystals (Press, 1981; Prager & Heidemann, 1997). In principle, the threefold symmetry of the indistinguishable protons ensures strict topological degeneracy in any crystal environment and tunnel effects are intrinsic to methyl groups. However, the splitting, which depends only on the potential barrier between indistinguishable configurations obtained by rotation of $\pm 2\pi/3$, may occur at any energy below the upper limit imposed by the rotational constant ($B \simeq 655\ \mu$eV). Tunnelling transitions above $\sim 1\ \mu$eV are best observed with the inelastic neutron scattering (INS) techniques. This is a very sensitive probe of the local potential.

In the crystalline state intra- and intermolecular contributions to the on-site potential can be distinguished. The former is determined by the structure of the chemical entity bearing the methyl group. The intermolecular potential depends on the molecular environment. In principle, these contributions can be related to the crystal structure *via ab initio* and molecular mechanics methods (Johnson *et al.*, 1997; Neumann & Kearley, 1997; Neumann & Johnson, 1997; Schiebel *et al.*, 1998; Nicolaï, Kaiser *et al.*, 1998; Nicolaï, Kearley *et al.*, 1998).

Table 1
Experimental details .

	14 K	300 K
Crystal data		
Chemical formula	$Mn(C_2H_3O_2)_2{\cdot}4D_2O$	$Mn(C_2H_3O_2)_2{\cdot}4D_2O$
Chemical formula weight	252.9	252.9
Cell setting, space group	Monoclinic, $P2_1/c$	Monoclinic, $P2_1/c$
a, b, c (Å)	10.88 (3), 17.39 (3), 9.04 (2)	11.10 (3), 17.51 (3), 9.09 (2)
α, β, γ (°)	90, 118.8 (2), 90	90, 118.6 (2), 90
V (Å^3)	1498.8	1551.2
Z	6	6
D_x (Mg m^{-3})	1.58	1.53
Radiation type	Neutron	Neutron
Wavelength (Å)	0.83080	0.8308
No. of reflections for cell parameters	14	14
θ range (°)	15.7–42.5	14.6–25
Temperature (K)	14	300
Crystal form, colour	Prism, pink	Prism, pink
Crystal size (mm)	3.0 × 3.0 × 3.0	3.0 × 3.0 × 3.0
Data collection		
Diffractometer	5C2, Orphée reactor (Saclay, France)	5C2, Orphée reactor (Saclay, France)
Data collection method	*DIF4N* (Stoe & Cie, 2000)	*DIF4N* (Stoe & Cie, 2000)
No. of measured, independent and observed parameters	7656, 6227, 4686	3536, 2222, 1570
Criterion for observed reflections	$I > 3.00\sigma(I)$	$I > 3.00\sigma(I)$
R_{int}	0.05	0.05
θ_{max} (°)	40	22.50
Range of h, k, l	$-17 \rightarrow h \rightarrow 3$ $0 \rightarrow k \rightarrow 26$ $-13 \rightarrow l \rightarrow 14$	$-12 \rightarrow h \rightarrow 4$ $-10 \rightarrow k \rightarrow 19$ $-9 \rightarrow l \rightarrow 10$
No. and frequency of standard reflections	2 every 450 min	2 every 450 min
Refinement		
Refinement on	F	F
$R[F^2>2\sigma(F^2)]$, $wR(F^2)$, S	0.0407, 0.0383, 1.0678	0.0657, 0.0456, 1.0655
No. of reflections and parameters used in refinement	4686, 380	1570, 314
Weighting scheme	Chebychev polynomial with four parameters (Carruthers & Watkin, 1979); 1.23, −1.20, 0.899, −0.290	Chebychev polynomial with five parameters (Carruthers & Watkin, 1979)
$(\Delta/\sigma)_{max}$	0.004947	0.068724
$\Delta\rho_{max}$, $\Delta\rho_{min}$ (fm Å^{-3})	1.37, −2.21	1.32, −1.5
Extinction method	Larson (1970), eq. (22)	Larson (1970), eq. (22)
Extinction coefficient	5.1 (4)	5.1 (4)

Computer programs used: *PRON* (modified version of *REDU*4; Stoe & Cie, 2000), M. Meven, *CRYSTALS* (Watkin, Prout, Carruthers & Betteridge, 1996), *Cameron* (Watkin, Prout & Pearce, 1996).

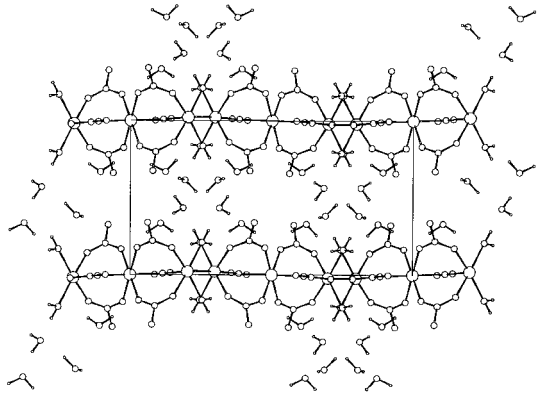

Figure 1
Crystalline structure of manganese diacetate tetrahydrate at 14 K. Representation in the (*ab*) plane.

However, there are large deviations between observed and calculated tunnelling frequencies, even with the most advanced methods. Therefore, tunnelling spectroscopy provides a crucial reference for an evaluation of the accuracy of the quantum chemistry methods.

Tunnelling transitions are best observed only at very low temperature (liquid helium) and usually disappear far below 100 K. Therefore, methyl dynamics and potential functions at high (room) temperature are largely unknown. The single-crystal neutron diffraction technique is unique to obtain proton density distributions at any temperature. In principle, modelling is necessary to unravel dynamical and statistical contributions. However, for methyl groups with intrinsic threefold degeneracy dynamical effects largely dominate the proton density distributions. This can be confirmed by comparison of the density distributions determined in the low-temperature regime to dynamics accurately known from tunnelling measurements.

We have thus undertaken extensive neutron diffraction and INS studies of the manganese(II) diacetate tetrahydrate, $[Mn(CH_3COO)_2]{\cdot}4H_2O$ crystal. The three tunnelling transitions observed at 1.2, 50 and 137 μeV (at 1.5 K, Heidemann *et al.*, 1985) were tentatively attributed to three crystallographic distinct methyl groups. The occurrence ratio of 1:1:1 is in accordance with the crystal structure at room temperature ($P2_1/c$ with Z = 6) determined by X-ray (van Niekerk & Schoening, 1953; Brown & Chidambaram, 1973; Bertaut *et al.*, 1974) and neutron diffraction (Tranqui *et al.*, 1977). However, the methyl dynamics are not yet fully understood. The rotational librations anticipated at 15, 8 and 6 meV are not visible and there is no satisfactory explanation for the unusual temperature dependence of the peak at 137 μeV (Heidemann *et al.*, 1985). Unfortunately, only the magnetic structure is known at low temperature (Burlet *et al.*, 1974; Schelleng *et al.*, 1968; Schmidt & Friedberg, 1969).

In this paper we present the crystal structure of manganese(II) diacetate tetrahydrate at 300 and 14 K determined by

Table 2
Refined parameters for the proton density of the methyl groups at room temperature.

The H distributions are represented with the model ring for free rotors: the position of the centre, the radius and the anisotropic thermal factor were refined. C—*R*C represents the distance between the carbon of the methyl group and the centre of the ring, C—H represents the distance between the carbon and the ring representing the H distributions. The corresponding tunnelling frequencies and potential barriers at low temperature are given for the sake of comparison.

	Ring centre (Å)	Radius (Å)	B (Å^2)	C—*R*C (Å)	C—H (Å)	Tunnelling (μeV)	V_3 (meV)
C2	X = 0.001 Y = 0.074 Z = 0.391	1.021	0.058	0.363	1.084	50	18.0
C4	X = 0.371 Y = 0.057 Z = −0.122	1.010	0.069	0.387	1.082	1.2	49.0
C6	X = −0.351 Y = 0.076 Z = −0.554	1.021	0.069	0.376	1.083	137	11.5

single-crystal neutron diffraction. The proton density distributions are presented for each methyl group. INS measurements performed on single crystals allow us to propose an assignment scheme for the tunnelling lines. The methyl dynamics are tentatively represented with molecular dynamics simulations. Finally, we propose a quantum model to account for both rotational dynamics and density distributions.

2. Experiments and calculations

Single crystals were pink transparent plates obtained by slow evaporation of saturated aqueous solutions. They are very fragile owing to easy cleavage along the (100) plane. Consequently, they were used as obtained. These crystals deteriorate rapidly outside an aqueous solution. The water molecules were deuterated in order to reduce incoherent diffusion.

We performed neutron diffraction experiments on the four-circle neutron diffractometer 5C2 at the LLB (Saclay, France). A lozenge-shaped crystal was glued on a goniometer head and oriented. At 14 K more than 7500 reflections were measured with the ω scan mode. The incident wavelength of 0.83 Å selected with the Cu (220) monochromator is shorter than that used in the previous work by Tranqui *et al.* (1977). The structure analysis was performed with the program *CRYS-*

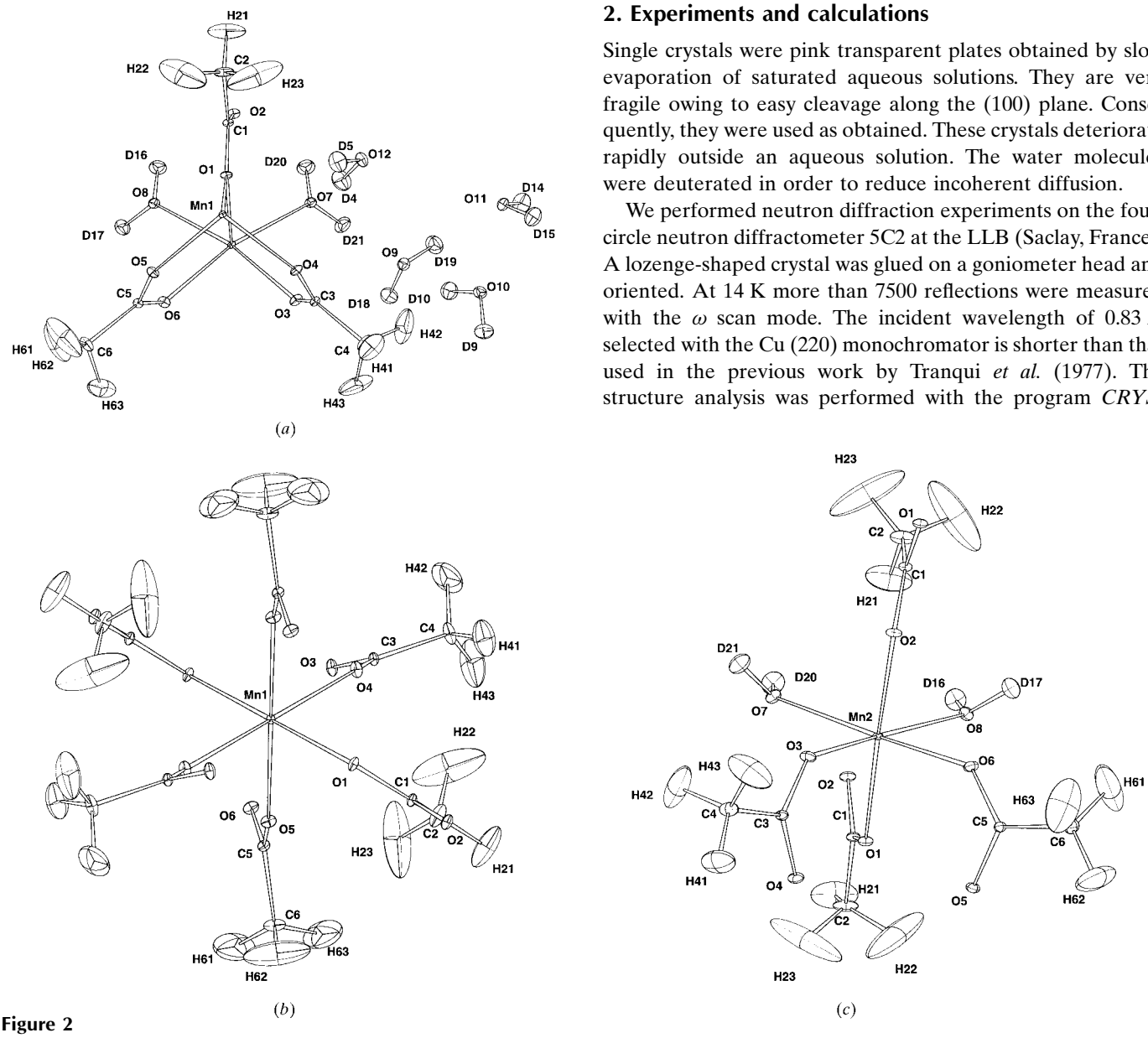

Figure 2
(*a*) Asymmetric unit and thermal ellipsoids at 14 K; (*b*) coordination polyhedron of Mn1 at 14 K; (*c*) coordination polyhedron of Mn2 at 14 K.

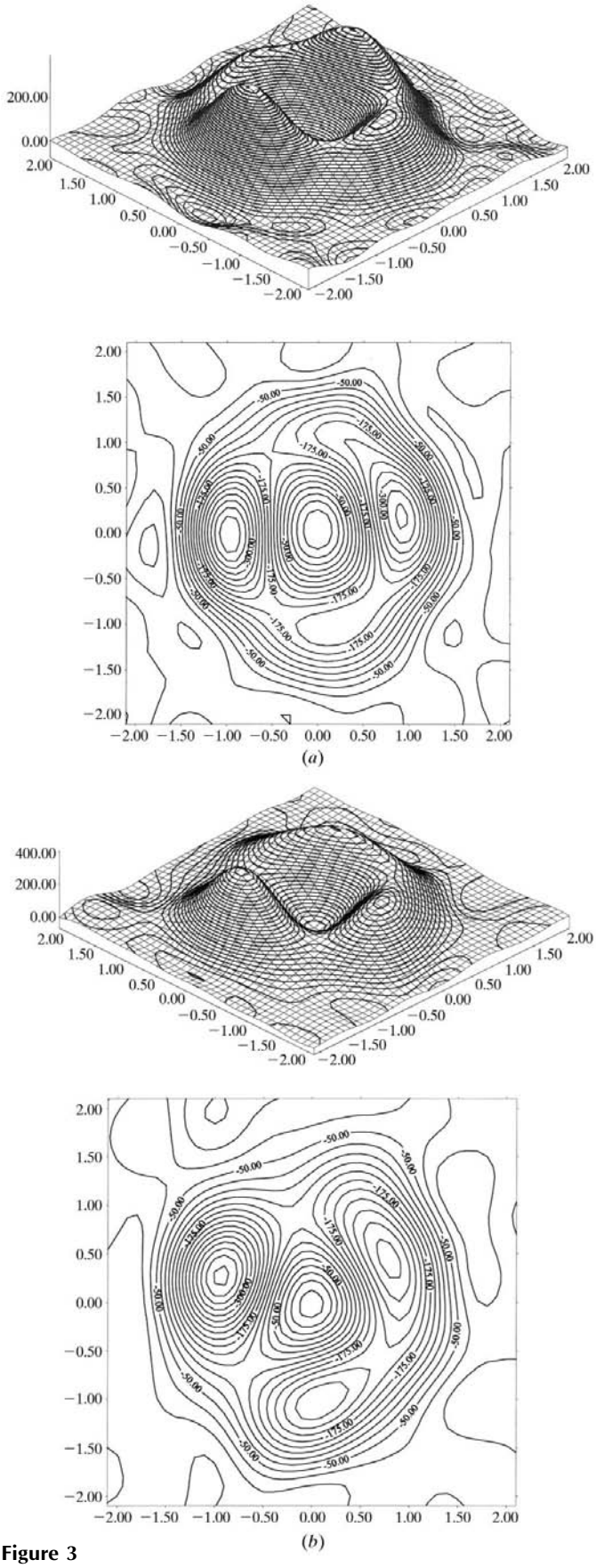

Figure 3
Experimental nuclear densities of the H atoms of the methyl groups at room temperature. Representation in the plane of rotation of the methyl groups. The nuclear densities, in fm Å^{-3}, correspond to the observed structure factors: (*a*) methyl group C2; (*b*) methyl group C4; (*c*) methyl group C6.

TALS (Watkin, Prout, Carruthers & Betteridge, 1996). The experimental details are listed in Table 1.

INS experiments were carried out at 1.7 K on the time-of-flight spectrometer IN5 at the ILL (Grenoble, France) with an incident wavelength of 9.8 Å. Two single crystals ($7 \times 5 \times 3$ mm^3 and $9 \times 6 \times 2$ mm^3, respectively) were measured. They were previously oriented on 5C2 in order to perform the INS measurements for momentum transfer parallel to the $(10\bar{1})$ and (100) crystallographic planes, respectively. They were glued on a goniometer head and loaded in a standard cryostat at the liquid helium temperature.

Molecular dynamics simulations were performed with the empirical pair-potential Universal Force Field (UFF; Rappe *et al.*, 1992) available in the commercial package *CERIUS*2 (Molecular Simulations Inc., 1996). Periodic boundary conditions and the Verlet algorithm were used to solve the classical equations of motion of all atoms. Atom trajectories were obtained by numerical integration of the Newton's equations. We performed molecular dynamics calculations at 150 K on a unit cell of manganese acetate. By analysing the atomic trajectories, we can construct the time-averaged atomic density and compare it to the experimental nuclear densities of the Fourier maps (Neumann & Kearley, 1997; Schiebel *et al.*, 1998).

Energy levels and wavefunctions for methyl quantum rotation were calculated with the variational method using basis sets of 40 free rotor wavefunctions, either odd or even.

3. Crystal structure

At room temperature: the space group is monoclinic $P2_1/c$ with $Z = 6$. There are three types of acetate groups, two inequivalent metal atoms and six crystallographically distinct water molecules (Figs. 1 and 2). There is no evidence for any phase transition between 300 and 14 K. Anisotropic displacements and geometric parameters at room temperature and 14 K have been deposited.[1]

Mn atoms are close to the *bc* plane. They are connected by Mn—O—Mn bonds and acetate bridges. Water molecules are between these planes. There are three different acetate bridges: Mn(1) and Mn(2) are linked *via* two distinct acetates and two Mn(2) are linked *via* the third type of acetate. The acetate entities are planar and bidentates. Each O atom is involved in a bond with a metallic atom and several hydrogen bonds with the surrounding water molecules.

The structure of the acetates are similar to those reported by Tranqui *et al.* (1977) at room temperature: in the acetate C1—C2, the C—O distances are quite different [we have measured at room temperature: C1—O1 1.278 (4) and C1—O2 1.245 (5) Å]. For the two other acetates the C—O distances are similar (∼1.26 Å). The angles O3—C3—O4 and O5—C5—O6 are 124.2 (3) and 123.6 (3)°, whereas O1—C1—O2 is 120.2 (3)°. These values compare to those at low temperature, 124.62 (6), 123.91 (7) and 120.64 (6)°, respectively. Each Mn atom is surrounded by a distorted octahedron of O atoms connected in the *bc* plane *via* their common acetate bridges and deuterium bonds with water molecules. The O—D distances in the water molecules vary between 0.9624 (18) and 0.9850 (15) Å at 14 K, and between 0.956 (9) and 0.984 (9) Å at room temperature.

4. Methyl groups

At room temperature, the Fourier maps for the proton distributions of the methyl groups are rather diffuse (see Fig. 3). The H distributions were represented with the ring model for free rotors. The position of the centre, the radius and an isotropic thermal factor were refined (Table 2). Compared to full refinement of H-atom positions, the number of parameters to be refined is reduced (314 instead of 379) and the *wR* factor is significantly better (4.56 rather than 7.00).

Significant departures from the free rotor model are observed. For the C4 methyl group the threefold symmetry suggests residual localization of the protons (Fig. 3*b*). The potential barrier should be much greater than the thermal energy. The C2 and C6 methyl groups give a ring of density, suggesting almost free rotation. However, two weak extrema of density for C2 and four of them with a square-like shape for C6 cannot be accounted for with either simple free rotors or threefold potentials. A similar distribution previously observed for the lithium acetate was interpreted in terms of coupling between rotation of the methyl group and translation of the centre of mass (Schiebel *et al.*, 1998).

At low temperature, the protons are rather well localized (see Fig. 4). The ring model is not adequate and full refinement of proton positions was performed. The C—H distances are between 1.042 (3) and 1.089 (2) Å. Proton densities for the C4 and C6 methyl groups correspond quite well to those anticipated for hindered rotors with rather high potential barriers and threefold symmetry. The more pronounced proton localization for C4, compared with C6, suggests a greater potential barrier.

The proton density of the C2 methyl group (Fig. 4*a*) is also compatible with localized protons, but significant deviation

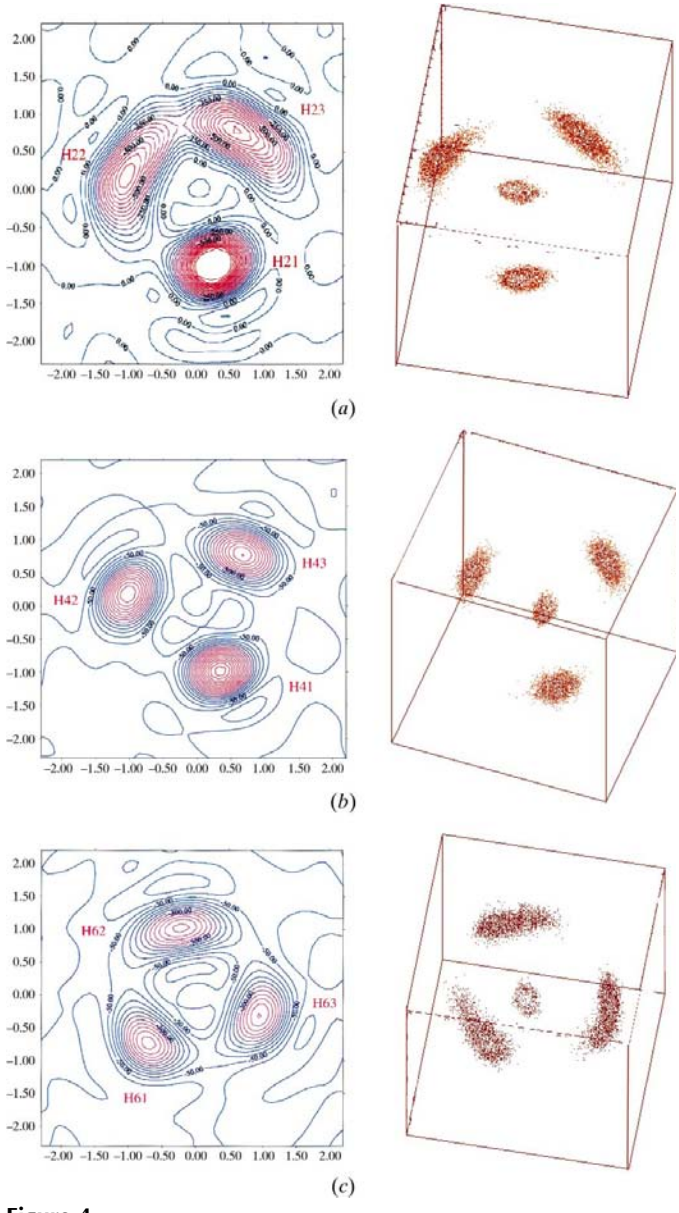

Figure 4
Comparison of the experimental proton densities, in fm Å^{-3}, at low temperature with the nuclear densities calculated from time-averaged simulations performed at 150 K. Representation in the plane of rotation of the methyl groups: (*a*) methyl group C2; (*b*) methyl group C4; (*c*) methyl group C6.

[1] Supplementary data for this paper are available from the IUCr electronic archives (Reference: LC0023). Services for accessing these data are described at the back of the journal.

from the ideal threefold symmetry appears. One proton, H21, is more localized than the others. We are not aware that any similar distribution had ever been reported.

5. Rotational dynamics

5.1. Assignment of the tunnelling lines

The most localized protons for the C4 methyl groups correspond to the largest potential barrier and, therefore, to the lowest tunnelling frequency at 1.2 μeV. However, it is not possible to assign the other two tunnelling frequencies by simple examination of the density distributions for C2 and C6. Therefore, further INS measurements were performed.

In the crystal, acetate entities are parallel to the (100) ($P2$), (001) ($P4$) and ($\bar{1}01$) ($P6$) planes, respectively. The axes of rotation for the methyl groups are aligned along different crystallographic directions. The INS intensity for a particular methyl group is a maximum for momentum transfer direction perpendicular to the rotational axis (Meinnel *et al.*, 1996; Nicolaï, Kaiser *et al.*, 1998). Therefore, the variation of the tunnelling peak intensities with the crystal orientation provides straightforward identification for each crystal site (see Table 2).

5.2. Classical molecular dynamics

Classical molecular dynamics simulations were performed to represent the methyl group dynamics. The universal force field is certainly not satisfactory and more accurate potential surfaces could be obtained with *ab initio* or DFT methods. However, regarding the rather complex structure of the Mn acetate and the rather large crystal unit cell, these methods require large computing capacity (Schiebel *et al.*, 1998). Furthermore, the main limitation of molecular dynamics is that simulations must be performed at high temperature (150 K in this work) in order to relax the system from the minimum of potential energy. Quantum effects are ignored and a uniform temperature of 150 K is a poor approximation to the zero-point energy of the crystal. Therefore, comparison with experiments performed at very low temperature is only suggestive. Further improvement of the calculated potential surface is of secondary importance compared to unavoidable crude approximations. Nevertheless, simulations may provide useful qualitative information on the probability distribution of heavy atoms (namely C and O) for which quantum effects can be largely ignored.

The atomic densities of the H and C atoms (Figs. 4*a*–*c*) are in qualitative agreement with the observation. The protons of the C4 methyl group are more localized than those of the C6 methyl. However, the estimated tunnelling frequencies are rather unrealistic.

Significant departure from the ideal threefold symmetry is clearly obtained for the protons of the C2 methyl group. The simulation reveals that this particular distribution could be related to the anisotropy of the displacements of the C2 atom: the calculated amplitude perpendicular to the *bc* plane is rather large. However, the distribution is quite different from that anticipated for a coupling between rotation and translation (Schiebel *et al.*, 1998).

5.3. Quantum dynamics

The Hamiltonian representing the rotational dynamics of a rigid methyl group can be written as

$$H = -(\hbar^2/2I_r)(\partial^2/\partial^2\varphi) + V(\varphi),$$

where I_r is the reduced moment of inertia of the rotor, φ the angular coordinate and $V(\varphi)$ the on-site potential. In the system under consideration only one tunnelling transition is known for each rotor and the Fourier series expansion is truncated to $V_3(1 - \cos 3\varphi)$. For a finite barrier height, each state splits into totally symmetric $\Psi_{\rm nA}$ and degenerate $\Psi_{\rm nE}$ states.

For those periodic potentials given in Table 2 eigenstates and wavefunctions are calculated numerically with basis sets of the free rotor wavefunctions. The density distribution is represented as a circular distribution with radius $r_0 \simeq 1$ Å. The amplitude depends on the sample temperature as

$$P(\varphi, T) = \sum_{n\sigma} \Psi^2_{n\sigma}(\varphi) \exp(-E_{n\sigma}/kT) / \sum_{n\sigma} \exp(-E_{n\sigma}/kT).$$

$P(\varphi,T)$ is convoluted with a radial static distribution

$$\rho(r) = (1/\pi u_r^2)^{1/2} \exp[-(r - r_0)^2/u_r^2],$$

where u_r^2 is comprised of the mean square amplitude for proton displacements (internal vibrations) and isotropic librations of the molecular entities.

The proton density distribution calculated for the C4 and C6 methyl groups at low temperature (Figs. 5*b* and *c*) are very similar to the observation. The proton localization is directly related to the potential barrier. The isotropic mean square displacement of 0.05 Å^2 is representative of the proton vibrations (∼0.01 Å^2) and molecular librations involving the methyl C atoms C4 or C6 (∼0.02 Å^2). The latter correspond roughly to oscillations around the centre of mass of the acetate entities, located at ∼1 Å from the methyl carbon. On the observed maps of proton density, librations are amplified by a factor of ∼1.52 determined by the distance of the proton plane to the C atom (∼0.5 Å). Our estimate of u_r^2 is thus compatible with the temperature factors derived from neutron diffraction.

The proton density distribution for the C4 methyl group (Fig. 5*a*) is well represented with a convolution of the density similar to those presented above with a distribution of the angular coordinate θ_L representing the rotation of the rigid methyl group with respect to H21. This angular distribution is due to large amplitude displacements perpendicular to the (001) mean plane suggested by molecular dynamics simulations. It is represented as

$$\rho(\theta_L) = (\langle\theta_L^2\rangle/2\pi)^{1/2} \exp(-\theta_L^2/\langle\theta_L^2\rangle).$$

The physical picture emerging from this map is quite unforeseen. It reveals that the potential minimum is much deeper for H21 that is well localized than for the other two protons. This is straightforward evidence that the three protons do not

experience the same local potential. (Indeed, this is not in conflict with the threefold symmetry of the rotational potential.) The distortion of the density confirms that the potential barrier for internal rotation is negligible compared with the depth of the local potential for H21. Our estimate of $\langle\theta_L^2\rangle$ = 0.06 rad^2 is compatible with a mean square amplitude of $\sim$0.03 Å^2 for C2 and an amplification factor of $\sim$2.

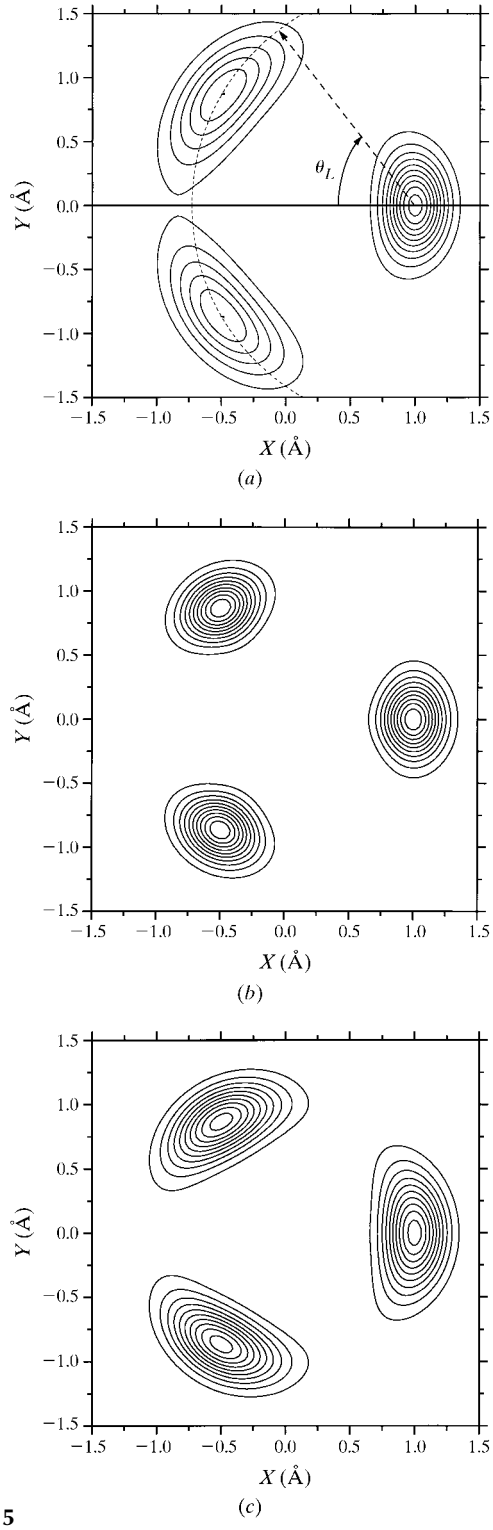

Figure 5
Calculated isocontour maps of proton densities at 14 K. (*a*) Methyl group C2: V_3 = 17.6 meV, u_r^2 = 0.05 Å^2, $\langle\theta_L^2\rangle$ = 0.06 rad^2; (*b*) methyl group C4: V_3 = 49 meV, u_r^2 = 0.05 Å^2; (*c*) methyl group C6: V_3 = 11.5 meV, u_r^2 = 0.05 Å^2.

The proton density distributions calculated at 300 K with the same potentials are very similar to those obtained at 14 K, apart from a broadening of the rotational wavefunctions. The distributions are quite different from the observed maps. There is a significant weakening of the potential barrier at room temperature.

For the C2 and C6 methyl groups the localization of the protons is no longer visible and these methyl groups can be regarded as free rotors. The density distributions are convoluted with anisotropic linear displacements whose mean-square amplitudes are u_x^2 and u_y^2. The two weak extrema for C2 (Fig. 6*a*) are due to anisotropic displacements along one direction, whilst the four extrema for C6 (Fig. 6*c*) are accounted for with the superposition of anisotropic displacements along two orthogonal directions.

5.4. Discussion

From previous calculations with various quantum mechanical methods it has been suggested that models based on methyl group rotation about a fixed axis are incorrect. Density distributions similar to those presented above have been regarded as suggesting coupling with molecular librational motions (Neumann & Kearley, 1997; Schiebel *et al.*, 1998). The angular coordinate of the methyl group and the translation of the centre of mass were supposed to be strictly correlated and proton motions were represented with cycloidal trajectories. Complex effective potentials and energy level schemes were proposed (Neumann & Kearley, 1997; Schiebel *et al.*, 1998).

This conclusion is quite questionable because dynamics cannot be extracted easily from the time-averaged atomic densities calculated at a rather high temperature within classical mechanics. These calculations may suggest some coupling, but they do not prove that it exists and effectively applies to tunnelling states. The classical view supposes that dynamics can be represented with atom trajectories. However, tunnelling is quantum mechanical in nature and atom trajectories are irrelevant. Only stationary states are observable. In the zero-order approximation we can distinguish eigenstates for methyl rotation on the one hand and for phonons on the other. Coupling terms may certainly exist and mix the zero-order states. However, the mixing decreases rapidly as the energy difference between levels increases. Since tunnelling appears in a frequency range at least one order of magnitude smaller than any optical phonon in molecular crystals, state mixing is negligible. In other words, on the tunnelling timescale the lattice can be represented with a static distribution of heavy atom positions. Simple convolution of the density distributions for quantum rotors and librations accounts for the observed proton density distributions.

It can be concluded that methyl dynamics and molecular librations largely dominate the observed density distributions and there is no need to suppose any correlation between these dynamics.

6. Conclusions

The crystal structure at low temperature of the manganese diacetate tetrahydrate confirms that the three tunnelling transitions correspond to three crystallographically inequivalent methyl groups. Each frequency is assigned to a particular crystal site by following the tunnelling intensities as a function of the crystal orientation. The proton probability densities for the C4 and C6 methyl groups derived from diffraction data at low temperature reveal the anticipated threefold symmetry. On the other hand, the proton distribution of the C2 methyl group shows large deviations from the ideal threefold symmetry. At room temperature the neutron diffraction technique provides a view of the proton distribution in a temperature range where tunnelling transitions are not observable. It appears that the effective potentials for the methyl groups are temperature dependent and almost vanish at room temperature. A weak threefold potential survives only for the most hindered group (C4).

The quantum mechanical approach offers a realistic representation of the observed densities with a rather limited number of parameters. Both dynamical and statistical effects determine the proton distribution. The potential barriers at low temperature are accurately determined by the tunnelling frequencies, even though the detailed potential shapes are unknown owing to the lack of observable librational transitions. The spatial extension of the squared rotational wavefunctions is comparable to the observed angular distributions. Convolution with static distributions representing librational dynamics occurring on much shorter timescales accounts for the various maps. Neutron diffraction offers clear evidence that effective rotational potentials are essentially intermolecular in nature. In this context, the lattice determines the rotational dynamics. However, the observed densities can be represented without any classical correlation between methyl rotation and lattice translation. The rotational potential is determined by the time-averaged crystal field.

The proton densities obtained with classical molecular dynamics simulations performed at 150 K emphasize the importance of molecular librations. Anisotropic librations with rather large amplitudes of the acetate entities bearing the C2 atom are compatible with the observed departure from threefold symmetry for the corresponding proton distribution.

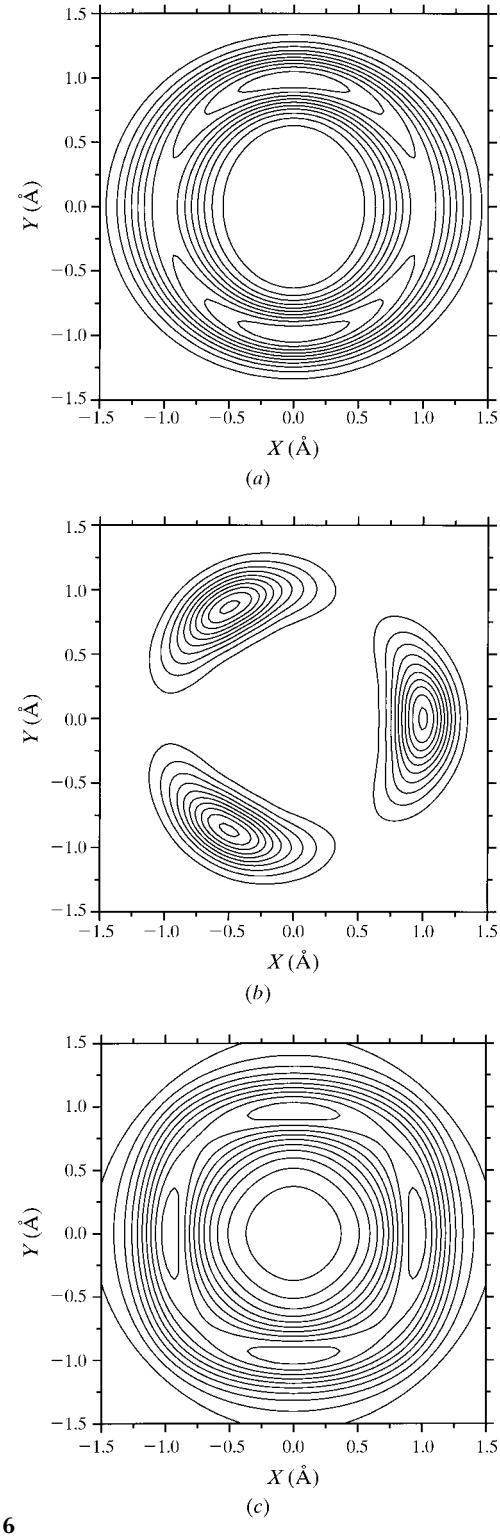

Figure 6
Calculated isocontour maps of proton densities at 300 K. (*a*) Methyl group C2: V_3 = 0 meV, $u_r^2 = u_x^2$ = 0.05 Å ^{2}; (*b*) methyl group C4: V_3 = 49 meV, u_r^2 = 0.05 Å^2; (*c*) methyl group C6: V_3 = 0 meV, u_r^2 = 0.05 Å ^{2}, $u_x^2 = u_y^2$ = 0.20 Å ^{2}.

We thank J. Goddard from the Parc d'Orsay (Orsay, France) for providing single crystals. We are also grateful to M. Neumann and M. R. Johnson from Institut Laue–Langevin (Grenoble, France) for helpful discussions.

References

Bertaut, E. F., Tran Qui, D., Burlet, P., Thomas, P. & Moreau, J. M. (1974). *Acta Cryst.* B**30**, 2234–2236.
Brown, G. M. & Chidambaram, R. (1973). *Acta Cryst.* B**29**, 2393–2403.
Burlet, P., Burlet, P. & Bertaut, E. F. (1974). *Solid State Commun.* **14**, 665–668.
Carruthers, J. R. & Watkin, D. J. (1979). *Acta Cryst.* A**35**, 698–699.
Heidemann, A., Clough, S., McDonald, P. J., Horsewill, A. J. & Neumaier, K. (1985). *Z. Phys. B*, **58**, 141–148.
Johnson, M. R., Neumann, M., Nicolaï, B., Smith, P. & Kearley, G. J. (1997). *Chem. Phys.* **215**, 343–353.
Larson, A. C. (1970). *Crystallographic Computing*, edited by F. R. Ahmed, pp. 291–294. Copenhagen: Munksgaard.

Meinnel, J., Carlile, C. J., Knigth, K. S. & Goddard, J. (1996). *Physica B*, **226**, 238–240.
Molecular Simulations Inc. (1996). *Cerius*2. BIOSYM/Molecular Simulations Inc., San Diego, CA 92121–3752, USA.
Neumann, M. & Johnson, M. R. (1997). *J. Chem. Phys.* **107**, 1725–1731.
Neumann, M. & Kearley, G. J. (1997). *Chem. Phys.* **215**, 253–260.
Nicolaï, B., Kaiser, E., Fillaux, F., Kearley, G. J., Cousson, A. & Paulus, W. (1998). *Chem. Phys.* **226**, 1–13.
Nicolaï, B., Kearley, G. J., Johnson, M. R., Fillaux, F. & Suard, E. (1998). *J. Chem. Phys.* **109**, 9062–9074.
Niekerk, J. N. van & Schoening, F. R. L. (1953). *Acta Cryst.* **6**, 227–232.
Prager, M. & Heidemann, A. (1997). *Chem. Rev* **97/8**, 2933–2966.
Press, W. (1981). *Springer Tracts Modern Physics*, Vol. 92. New York: Springer Verlag.
Rappe, A. K., Casewitt, C. J., Colwell, K. S., Goddard, W. A. & Skiff, W. M. (1992). *J. Am. Chem. Soc.* **113**, 10024–10035.
Schelleng, J. H., Raquet, C. A. & Friedberg, S. A. (1968). *Phys. Rev.* **176**, 708–722.
Schiebel, P., Kearley, G. J. & Johnson, M. R. (1998). *J. Chem. Phys.* **108**, 2375–2382.
Schmidt, V. A. & Friedberg, S. A. (1969). *Phys. Rev.* **188**, 809–812.
Stoe & Cie (2000). *DIF*4*N. Modified Linux Version of STOE Four-circle Diffractometer Control Program*. Stoe & Cie GmbH, D 64295 Darmstadt, Germany.
Tranqui, D., Burlet, P., Filhol, A. & Thomas, M. (1977). *Acta Cryst.* B**33**, 1357–1361.
Watkin, D. J., Prout, C. K., Carruthers, J. R. & Betteridge, P. W. (1996). *CRYSTALS*, Issue 10. Chemical Crystallography Laboratory, Oxford, England.
Watkin, D. J., Prout, C. K. & Pearce, L. J. (1996). Chemical Crystallography Laboratory, Oxford, England.